Available online at www.sciencedirect.com
SCIENCE DIRECT
Journal of Catalysis 237 (2006) 426–430
JOURNAL OF CATALYSIS
www.elsevier.com/locate/jcat

Research Note

Surface structure effects in nanocrystal MnO_2 and Ag/MnO_2 catalytic oxidation of CO

Run Xu, Xun Wang, Dingsheng Wang, Kebin Zhou, Yadong Li *

Department of Chemistry and the Key Laboratory of Atomic & Molecular Nanosciences (Ministry of Education, China), Tsinghua University, Beijing 100084, PR China

Received 4 July 2005; revised 22 October 2005; accepted 25 October 2005

Abstract

Pure-phase α-MnO_2 and β-MnO_2 nanowires/nanorods were synthesized through an easy solution-based hydrothermal method, and the effect of the manganese dioxide phase on the activity of MnO_2 and Ag/MnO_2 for the oxidation of CO was investigated. MnO_2 is an effective catalyst in CO oxidation, and its activity depends on the crystal phase of MnO_2. α-MnO_2 exhibits a higher activity than β-MnO_2, because the α-MnO_2 nanowires can be reduced more easily than the β-MnO_2 nanorods. Moreover, when Ag was introduced to MnO_2, a strong interaction occurred between Ag and MnO_2. The catalytic activity clearly correlates with this interaction, which is determined by crystal phase and surface structure.

Keywords: MnO_2 nanocrystal; Controlled-synthesis; Crystal phase; CO oxidation

1. Introduction

The performance of catalysts depends strongly on their surface structure and surface active sites, which have a direct relationship with the crystal planes, crystal phases, and stereochemistry of catalysts [1,2]. A typical case is iron catalysts used for the synthesis of ammonia, for which the reaction rate on the {111} planes is more than 400 times higher than that on the {110} planes and roughly 15 times higher than that on the {100} planes [1,3]. Bell et al. [4–7] reported that different crystal phases of zirconia-supported copper catalysts exhibit different activity for the synthesis of methanol, and the catalyst prepared on monoclinic-ZrO_2 is 7.5 times more active than that prepared on tetragonal-ZrO_2. Consequently, a feasible approach to designing and constructing catalysts with high activity and selectivity may be through the controllable synthesis of catalyst materials with well-defined crystal planes or crystal phases. We recently reported that using an easy solution-based hydrothermal method, CeO_2 nanorods exposing mostly {001} and {110} planes can be synthesized; these CeO_2 nanorods show higher catalytic activity for CO oxidation than CeO_2 nanoparticles [8,9]. Morphology-controlled synthesis of nanomaterials may present an opportunity for the synthesis of catalytic materials with desired properties, because these novel materials nucleate and grow in an epitaxial manner [10,11].

CO oxidation is an important process in three-way catalysis for the treatment of exhaust gas from automobiles and in selective oxidation of CO in reformer gas for fuel cell applications [12]. Precious metals, such as Au, Pt, and Pd, have high activity and stability for the oxidation of CO [13,14]. Recently, considerable research has focused on base metal catalysts for CO oxidation, because of the limited availability of precious metals. Manganese dioxides and derivative compounds have attracted special attention and have been widely used as catalysts and catalyst supports due to their redox capabilities [15,16]. These redox capabilities are strongly enhanced when other elements are combined [17]. Imamura et al. [15] reported that Ag–Mn composite oxides exhibited high activity for CO oxidation. A combination of Ag and Mn seems to be an important contributing factor to catalytic activity [18,19], but details of the action of Ag and Mn in these catalysts are not yet available. The main reason for this may be that the performance of the manganese oxides for those applications is critically controlled by their phase composition and textural properties,

* Corresponding author. Fax: +86 10 62788765.
E-mail address: ydli@mail.tsinghua.edu.cn (Y. Li).

0021-9517/$ – see front matter
doi:10.1016/j.jcat.2005.10.026

which depend largely on the preparation method [20]. Different structural forms of MnO_2 including α, β, γ, and δ types, exist in nature. The crystallographic forms are generally believed to be responsible for their properties. The synthesis of manganese oxides with well-controlled dimensionality, size, and crystal structure is very difficult by conventional catalyst preparation methods. We previously reported a successful method for synthesizing α-, β-, γ-, and δ-MnO_2, which have a well-defined single-crystalline nanostructure [21]. The present work is concerned with the catalytic activity of α-MnO_2 and β-MnO_2 nanowires/nanorods in CO oxidation and a comparative study of α-MnO_2 and β-MnO_2 as a support for Ag catalysts.

2. Experimental

Synthesis of MnO_2 nanowires/nanorods was performed by hydrothermal method as described previously [21]. The Ag/MnO_2 catalysts with 15 wt% Ag loading were prepared by an incipient wetness impregnation method. The prepared MnO_2 nanowires/nanorods were impregnated with an aqueous solution of $AgNO_3$ under vigorous stirring, followed by drying to remove the solvent. The obtained sample was calcined at 350 °C for 3 h.

The BET surface areas of the catalysts were determined by N_2 adsorption at −196 °C using a Tristar 2010 Chemical Adsorption Instrument (Micromeritics). X-Ray diffraction (XRD) studies were performed with a Bruker D8 Advance X-ray diffractometer with monochromatized Cu-K_α radiation ($\lambda = 1.5418$ Å). The nanostructural product was further examined with transmission electron microscopy (TEM; Hitachi H-1200, Tokyo, Japan).

Temperature-programmed reduction (TPR) was carried out in a U-tube quartz reactor. The samples (40 mg) were flushed with a nitrogen flow of 50 mL min^{-1} at 120 °C to remove water and then reduced in a flow of hydrogen–nitrogen mixture (containing 5 vol% of hydrogen) at a rate of 10 °C min^{-1}. Hydrogen consumption was monitored by a thermal conductivity cell attached to a gas chromatograph.

The catalytic activities for CO oxidation were evaluated in a fixed-bed quartz tubular reactor. The catalyst particles (0.15 g) were placed in the reactor. The reactant gases (1.0% CO, 16% O_2, balanced with nitrogen) passed through the reactor at a flow rate of 100 mL min^{-1}. The products were analyzed by a gas chromatograph equipped with a TDX column.

3. Results and discussion

3.1. BET, XRD, and TEM analysis

The BET surface area of α-MnO_2 nanowires is higher than that of β-MnO_2 nanorods (Table 1). When Ag was introduced onto α-MnO_2 and β-MnO_2, the surface areas decreased. XRD results indicate that pure α- and β-MnO_2 crystal phase can be obtained under current synthetic conditions (Fig. 1). For the Ag/α-MnO_2 sample, the XRD pattern was similar to the precursor, suggesting that Ag is finely dispersed on the MnO_2

Table 1
Comparison of CO oxidation on manganese dioxide

Catalysts	BET surface area ($m^2\ g^{-1}$)	T_{90} (°C)[a]	Specific rate ($mol_{CO}\ m_{cat}^{-2}\ s^{-1} \times 10^{-8}$)
α-MnO_2	80.6	126	4.21[b]
β-MnO_2	55.7	169	2.10[b]
Ag/α-MnO_2	64.2	90	7.74[c]
Ag/β-MnO_2	40.0	80	16.33[c]

[a] The temperature at 90% conversion.
[b] The reaction temperature is 130 °C.
[c] The reaction temperature is 80 °C.

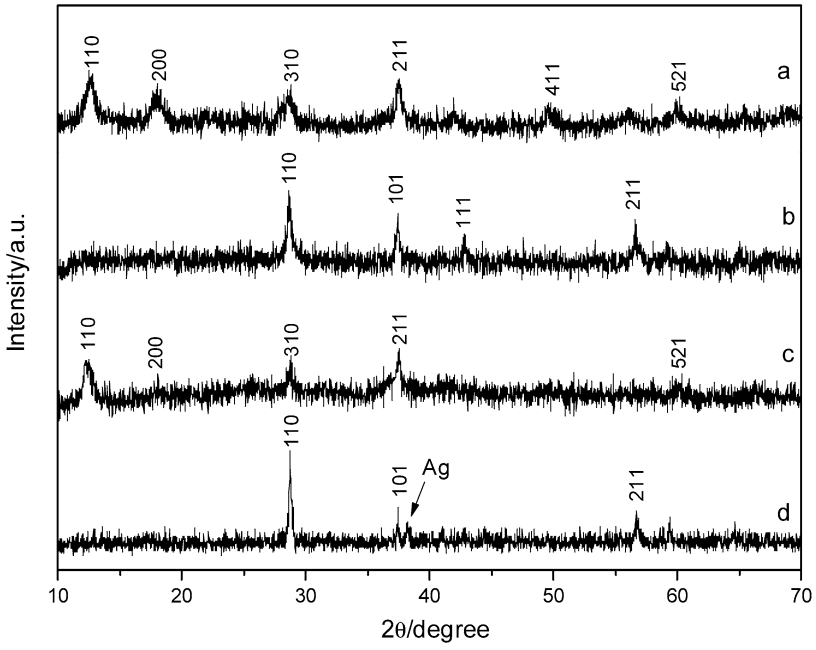

Fig. 1. XRD patterns of (a) α-MnO_2 nanowires; (b) β-MnO_2 nanorods; (c) Ag/α-MnO_2 nanowires; (d) Ag/β-MnO_2 nanorods.

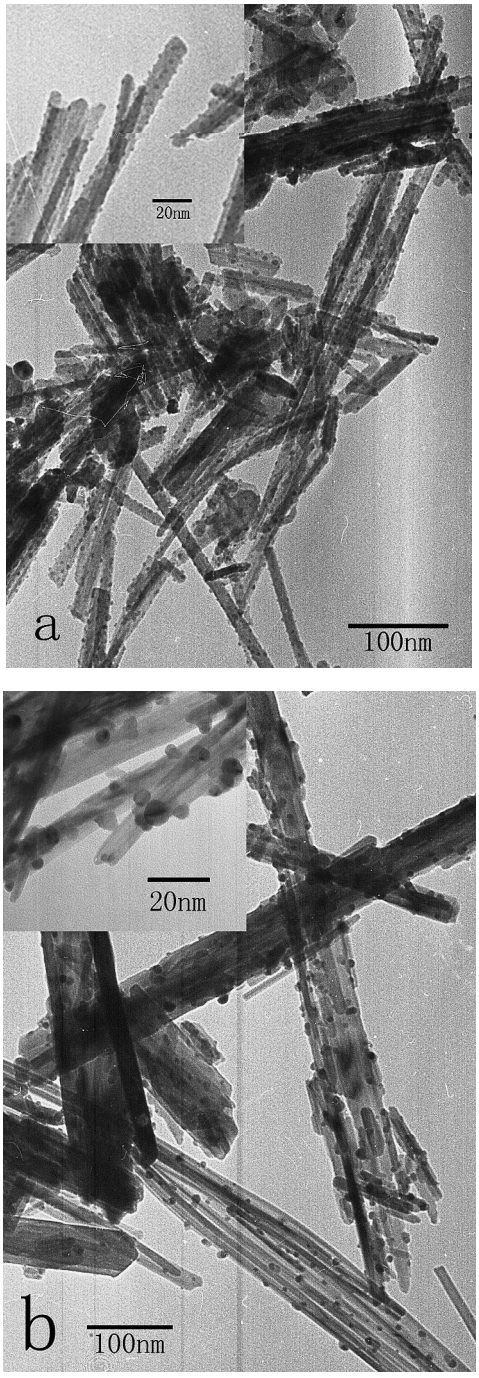

Fig. 2. TEM images of (a) Ag/α-MnO_2 nanowires; (b) Ag/β-MnO_2 nanorods.

supports. A weak diffraction peak corresponding to Ag crystal phase could be observed on the XRD of Ag/β-MnO_2 sample.

The as-prepared α-MnO_2 and β-MnO_2 samples have ribbonlike nanowire and nanorod morphology (see supporting information). Fig. 2 shows representative TEM images of Ag catalysts supported on α-MnO_2 nanowires and β-MnO_2 nanorods, respectively. The inset in the upper left shows a magnified view of the Ag particles, illustrating that the distribution of Ag particles on the supports is rather uniform. The Ag particles in these catalysts are near-spherical in shape, whereas the MnO_2 keeps its nanowire/nanorod morphology. The mean particle size for

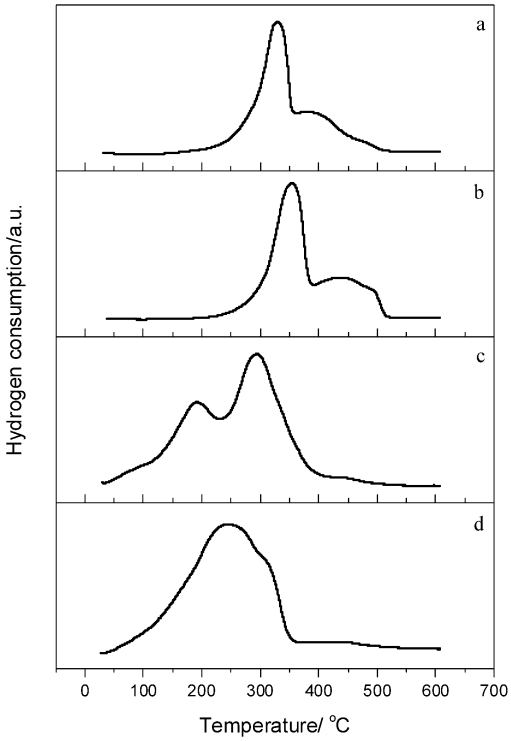

Fig. 3. TPR profiles of (a) α-MnO_2 nanowires; (b) β-MnO_2 nanorods; (c) Ag/α-MnO_2 nanowires; (d) Ag/β-MnO_2 nanorods.

Ag dispersed on α-MnO_2 nanowires is about 2–6 nm, and that for Ag dispersed on β-MnO_2 nanorods is 5–10 nm.

3.2. TPR analysis of MnO_2 and Ag/MnO_2

Fig. 3a presents the TPR profile of the α-MnO_2 nanowires. Two peaks of H_2 consumption are observed at 330 and 389 °C, and the ratio of the low-temperature peak to the high-temperature peak is about 2. Because the initial species is MnO_2 (see the XRD patterns), we believe that the low-temperature peak should be attributed to the reduction of MnO_2 to Mn_3O_4, whereas the high-temperature peak should be attributed to the reduction of Mn_3O_4 to MnO [22]. The TPR profile of the β-MnO_2 nanorods is similar to that of the α-MnO_2 nanowires, but is shifted slightly to higher temperatures (Fig. 3b). This finding indicates that the α-MnO_2 nanowires are more easily reduced than the β-MnO_2 nanorods.

Compared with those of the α-MnO_2 nanowires, the TPR peaks of the Ag/α-MnO_2 sample shifted to lower temperatures and exhibited a higher intensity of the peak at higher temperatures (Fig. 3c). The results demonstrate that Ag enhanced the reduction of the α-MnO_2 nanowires and that a strong interaction between Ag and MnO_2 occurred. When Ag was introduced on the β-MnO_2 nanorods, the reduction behavior differed from that observed on the Ag/α-MnO_2. A wide and asymmetric peak was detected at 245 °C, along with a small shoulder at about 312 °C. This indicates that the MnO_2 was probably reduced to MnO without the formation of intermediate Mn_3O_4. Ag enhanced the reduction of MnO_2 through the spillover of hydrogen from silver atoms to manganese oxides [15]. A strong

interaction between Ag and MnO_2 favors the spillover of hydrogen and its subsequent reaction with the MnO_2; thus, a stronger metal–support interaction in Ag/β-MnO_2 nanorods is detected.

3.3. Catalytic activity for CO oxidation

Catalytic activity measurements of CO oxidation on as-prepared MnO_2 and Ag/MnO_2, given in Table 1, demonstrate that the α-MnO_2 nanowires were more active than the β-MnO_2 nanorods. The percentage CO conversion reached 90% at 126 °C on α-MnO_2 and at 169 °C on the β-MnO_2 nanorods. The specific reaction rate on the α-MnO_2 nanowires was twice as high as that on the β-MnO_2 nanorods at 130 °C. The presence of Ag greatly improved the catalytic activity for CO oxidation. The percentage CO conversion on Ag/α-MnO_2 and Ag/β-MnO_2 all reached 90% at $<$100 °C. It is noteworthy that the reaction rate on Ag/β-MnO_2 at 80 °C was more than twice that on the Ag/α-MnO_2 catalyst. Compared with β-MnO_2 nanorods, the T_{90} of Ag/β-MnO_2 was decreased by 89 °C. Thus, Ag enhances the catalytic activity on manganese oxides and is more efficacious for β-MnO_2 nanorods.

Generally, CO oxidation on transition metal oxides, such as MnO_x, CeO_2, Co_3O_4, Fe_2O_3, and CuO, follows a mechanism proposed by Mars–van Krevelen [23] implying that lattice oxygen incorporation occurs during CO oxidation and that the reduced surface of the metal oxide is rejuvenated by taking up oxygen from the feed mixture [24,25]. On the other hand, it is well known that the reactivity for structure sensitive reaction depends on the particle size, morphology, and crystal plane of the catalyst [1,2,26]. Therefore, the surface structure of the catalyst greatly influences catalytic performance.

α- and β-MnO_2 are both constructed from chains of {MnO_6} octahedra, which are linked in different ways. In α-MnO_2, each octahedron shares two edges with those of the neighboring chain. It consists of an hcp anionic lattice and contains two different kinds of oxygen atoms, one at the center of an almost equilateral triangle of cations Mn^{4+}, indicating a sp^2 hybridization with bond distances to Mn of 1.86 and 1.91 Å, and the other at the apex of a trigonal pyramid of cations, indicating a sp^3 hybridization with bond distances to Mn of 1.89 and 1.92 Å [27]. β-MnO_2 has a rutile structure, with the oxygen atoms forming a slightly distorted hexagonal closely packed (hcp) array. The basic motif of this tetragonal structure is an infinite chain of octahedra-sharing opposite edges, with each chain corner-linked with four similar chains. All octahedra are equivalent, and the average Mn–O distance is 1.88 Å [28]. Therefore, the structure of β-MnO_2 is denser than that of α-MnO_2, whereas the activity of the lattice oxide of β-MnO_2 is predicted to be lower than that of the lattice oxide of α-MnO_2. High-resolution TEM results and structure analysis in theory reveal that α-MnO_2 has an "noncompact" structure, making the rupture of the O–Mn bond easier in α-MnO_2 than in β-MnO_2. In this regard, α-MnO_2 and β-MnO_2 have different catalytic activities corresponding to their different surface structures.

Introducing Ag to MnO_2 produces a strong Ag–MnO_2 interaction. The surface structure clearly determines the intensity of interaction and thus the catalytic activity. Imamura et al. [15] reported that the catalytic activity of CO oxidation on Ag–Mn composite oxides depends on the interaction between Ag and Mn. The active oxygen on Ag is consumed mainly in the oxidation of CO, and Mn serves as an oxygen carrier [18]. Moreover, strong interaction favors the oxygen spillover from Mn to Ag and improves catalytic activity. This is agreement with the TPR results, which indicate that the interaction between Ag and MnO_2 decreased the reduction temperature of β-MnO_2. Based on this, a stronger interaction between metal and supports occurred in Ag/β-MnO_2 and an enhanced catalytic activity was found, similar to that for Au/CeO_2 and Au/CuO as reported recently [29,30].

4. Conclusion

Different structures of MnO_2 catalysts (α- and β-type nanowires/nanorods) were synthesized by an easy solution-based hydrothermal method. The single-crystal α-MnO_2 and β-MnO_2 nanowires/nanorods were used as CO oxidation catalysts in an attempt to gain insight into how the crystal phase and surface structure influence the oxidation reaction. α-MnO_2 has a "noncompact" structure that can be reduced at lower temperatures. Thus, α-MnO_2 nanowires show higher CO oxidation activity than β-MnO_2 nanorods. Introducing Ag onto MnO_2 produced a strong Ag–MnO_2 interaction. The catalytic activity clearly correlates with this interaction, which is determined by crystal phase and surface structure. This study provides an example of how to design catalytic materials through a morphology-controlled synthesis method and how to use these materials as model catalysts in laboratory investigations as well as practical applications.

Acknowledgments

This work was supported by the NSFC (grants 90406003, 50372030, 20401010, and 20131030), the Foundation for the Author of National Excellent Doctoral Dissertation of the People's Republic of China, and the State Key Project of Fundamental Research for Nanomaterials and Nanostructures (2003CB716901).

Supporting information

This article contains additional supporting information. Please visit doi: 10.1016/j.jcat.2005.10.026.

References

[1] G.A. Somorjai, The surface science of heterogeneous catalysis, in: Proceedings of the Robert A. Welch Foundation Conferences on Chemical Research, Houston, Texas, November 9–11, 1981, in: Heterogeneous Catalysis, vol. XXV, 1981, pp. 83–127.
[2] P.L.J. Gunter, J.W. Niemantsverdriet, F.H. Ribeiro, G.A. Somorjai, Catal. Rev. Sci. Eng. 39 (1997) 77.
[3] G. Ertl, Primary steps in ammonia synthesis, in: Proceedings of the Robert A. Welch Foundation Conferences on Chemical Research, Houston, Texas, November 9–11, 1981, in: Heterogeneous Catalysis, vol. XXV, 1981, pp. 179–207.

[4] K.T. Jung, A.T. Bell, Catal. Lett. 1–2 (2002) 63.
[5] K. Pokrovski, K.T. Jung, A.T. Bell, Langmuir 17 (2001) 4297.
[6] M.D. Rhodes, A.T. Bell, J. Catal. 233 (2005) 198.
[7] M.D. Rhodes, K.A. Pokrovski, A.T. Bell, J. Catal. 233 (2005) 210.
[8] K.B. Zhou, X. Wang, X.M. Sun, Q. Peng, Y.D. Li, J. Catal. 229 (2005) 206.
[9] K.B. Zhou, R. Xu, X.M. Sun, H.D. Chen, Q. Tian, D.X. Shen, Y.D. Li, Catal. Lett. 101 (2005) 169.
[10] X. Wang, Y.D. Li, Angew. Chem. Int. Ed. 41 (2002) 4790.
[11] Y.N. Xia, P.D. Yang, Y.G. Sun, Y.Y. Wu, B. Marers, B. Gates, Y.D. Yin, F. Kim, H.Q. Yan, Adv. Mater. 15 (2003) 353.
[12] F. Kapteijn, L. Singoredjo, A. Andreini, Appl. Catal. B 3 (1994) 173.
[13] S.D. Gardner, G.B. Hoflund, B.T. Upchurch, D.R. Schryer, E.J. Kielin, J. Schryer, J. Catal. 129 (1991) 114.
[14] D.R. Schryer, B.T. Upchurch, J.D. Van Norman, K.G. Bromn, J. Schryer, J. Catal. 122 (1990) 193.
[15] S. Imamura, H. Sawada, K. Uemura, S. Ishida, J. Catal. 109 (1988) 198.
[16] R. Lin, W.-P. Liu, Y.-J. Zhong, M.-F. Luo, Appl. Catal. A 220 (2001) 165.
[17] M. Haruta, N. Yamada, T. Kobayashi, S. Lijima, J. Catal. 115 (1989) 301.
[18] M.-F. Luo, X.-X. Yuan, X.-M. Zheng, Appl. Catal. A 175 (1998) 121.
[19] K.S. Song, S.K. Kang, S.D. Kim, Catal. Lett. 49 (1997) 65.
[20] J. Boyero Macstre, E. Fernández López, J.M. Gallardo-Amores, R. Ruano Casero, V. Sánchez Escribano, E. Pérez Bernal, Int. J. Inorg. Mater. 3 (2001) 889.
[21] X. Wang, Y.D. Li, Chem. Eur. J. 9 (2003) 300.
[22] H. Trevino, G.D. Lei, W.M.H. Sachtler, J. Catal. 154 (1995) 245.
[23] J. Jansson, J. Catal. 194 (2000) 55.
[24] S.K. Kulshreshtha, M.M. Gadgil, Appl. Catal. B 11 (1997) 291.
[25] A.M. Duprat, P. Alphonse, C. Sarda, A. Rousset, B. Gillot, Mater. Chem. Phys. 37 (1994) 76.
[26] M. Boudart, Adv. Catal. Relat. Subj. 20 (1969) 153.
[27] M.M. Thackeray, Prog. Solid State Chem. 25 (1997) 1.
[28] Y. Chabre, J. Pannetier, Prog. Solid State Chem. 23 (1995) 1.
[29] A.M. Venezia, G. Pantaleo, A. Longo, G.D. Carlo, M.P. Casaletto, F.L. Liotta, G. Deganello, J. Phys. Chem. B 109 (2005) 2821.
[30] G. Glaspell, L. Fuoco, M.S. El-Shall, J. Phys. Chem. B 109 (2005) 17350.